2008 IEEE International Conference on
Robotics and Automation
Pasadena, CA, USA, May 19-23, 2008

Boundary Following by Robot Formations without GPS

Fumin Zhang and Salman Haq

Abstract— **We design sensing algorithms and a control law for a group of mobile robots to follow a boundary curve without utilizing a global positioning system (GPS). The sensing algorithms allow each robot to estimate the shape and the orientation of the entire formation from readings of range sensors and a speedometer. The usage of GPS is avoided because each robot is able to estimate the relative position of the entire formation with respect to the boundary curve. Based on these estimates, we present a control law that allows the robot formation to achieve desired non-singular shape while following the boundary curve. We control the distance between the center of mass of the formation and the boundary curve so that it converges to desired value. Our control law also guarantees that there will be no collision between any pair of robots and no collision between any robot and the boundary curve.**

I. Introduction

Navigation, path planning, and obstacle avoidance are fundamental research problems for mobile robotics. In [1], a boundary following strategy was developed for single robot to avoid obstacles and reach a target. This work, together with later developments such as [2], [3], established boundary following as a viable approach for online navigation and obstacle avoidance. One significant benefit for the boundary following approach is that a robot may plan its motion based on measurements of the boundary, without using any form of a global positioning system (GPS). This advantage is desired for applications where GPS is not available or can be easily disturbed.

Significant recent developments have been achieved in navigating multiple robots cooperatively. In [4]–[10], various algorithms and control methods are developed for robot teams to move to a target and/or avoid obstacles along the way. These results require information from a GPS to achieve desired formations. Even though the boundary following methods for single robot may be combined with the formation control laws, the benefit of not requiring GPS is lost.

F. Zhang is with School of Electrical and Computer Engineering, Georgia Institute of Technology, Savannah, GA 31407. Email: fumin@ece.gatech.edu.

S. Haq is with Advanced Simulation Technology, Inc 500A Huntmar Park Dr., Herndon, Va 20170. Email: salman.haq@asti-usa.com

The authors want to thank P. S. Krishnaprasad and E. W. Justh for collaboration and guidance and thank N. E. Leonard for discussions and support. This research was supported in part by the National Aeronautics and Space Administration under NASA-GSFC Grant No. NAG5-10819, by the Air Force Office of Scientific Research under AFOSR Grant No. F49620-01-0415, by the Army Research Office under ODDR&E MURI97 Program Grant No. DAAG55-97-1-0114 to the Center for Dynamics and Control of Smart Structures (through Harvard University), and under ODDR&E MURI01 Program Grant No. DAAD19-01-1-0465 to the Center for Communicating Networked Control Systems (through Boston University).

In this paper, we develop sensing algorithms and control laws so that a team of robots are able to perform boundary following without GPS. Our method is based on the establishment of a shape theoretic approach in formation control which does not depend on GPS. Shape theory is established by physicists and statistician for measuring configurations of clusters of particles [11]–[14]. Some recent work [15], [16] applied the shape theory to cooperative control for robot formations. Results in this paper extend previous work by completely eliminating the requirements for GPS and by combining the shape controller design with boundary following control to provide an integrated navigation method with provable convergence.

In section II, we introduce the algorithms that measure the shape, orientation, and position of the formation based on shape theory. We then develop the relative motion dynamics of the entire formation with respect to a boundary curve in section III. A controller for formation keeping, curve tracking, and obstacle avoidance is introduced and justified in section IV. Simulation results that demonstrate formation shape changes while moving along an elliptic boundary are shown in V.

II. Formation Shape, Orientation, and Position

For motion planning purposes, we model robots as point particles. Suppose each particle has unit mass and there are N particles in a formation. This formation can be described in a lab coordinate frame with $\mathbf{r}_i \in \mathscr{R}^2$ as the position of the ith particle. The velocity of each particle is $\dot{\mathbf{r}}_i \in \mathscr{R}^2$. A global positioning system (GPS) is required to determine the positions and the velocities in the lab coordinate system.

In this paper, we discuss the situation that a GPS is not available. In replacement of the GPS, we make the following assumptions on the sensing ability of each robot:

1) Each robot is equipped with range sensors (e.g. laser range finders or sonars) that have a 360 degree of view. To simplify our discussion, suppose the sensors are powerful enough to cover the full workspace.
2) Each robot has a speedometer which measures its speed. Note that the direction of motion is not known.

When a sensor ray is blocked by another robot, the distance between the two robots can be determined. Let α be the angle index of the sensor rays. Knowing α and the relative distances allows each robot to measure the relative displacement vectors between itself and all other robots in the formation. These relative vectors determine the formation shape. Furthermore, each robot is able to attach a right handed coordinate frame to the entire formation. An example is shown in Figure 1, where the relative vector $(\mathbf{r}_2 - \mathbf{r}_1)$ is

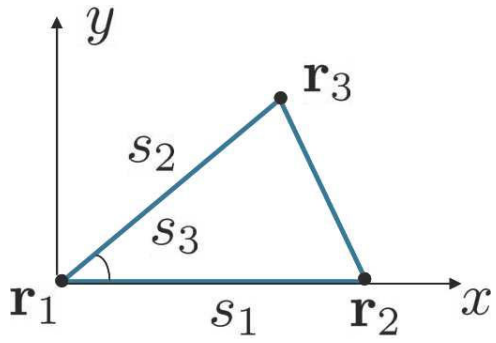

Fig. 1. A gauge convention and a set of shape variables chosen to describe a triangular formation. The x axis is aligned with $(\mathbf{r}_2 - \mathbf{r}_1)$. s_1 is the distance between $\mathbf{r}_2$ and $\mathbf{r}_1$, s_2 is the distance between $\mathbf{r}_3$ and $\mathbf{r}_1$, and s_3 is the angle between $(\mathbf{r}_2 - \mathbf{r}_1)$ and $(\mathbf{r}_3 - \mathbf{r}_1)$.

always aligned with the horizontal axis of this frame, and the vertical y-axis is perpendicular to the horizontal x-axis. We call the procedure to establish such a coordinate frame a *gauge convention*. Different robot may choose different gauge conventions and they do not necessarily know what gauge conventions other robots have chosen. For this reason we call the coordinate frame chosen by robot i the ith frame.

Now suppose there is a stationery obstacle with a smooth boundary curve in the workspace. We show that each robot can determine the orientation and position of the formation relative to this boundary curve. The key idea is to find the point on the boundary curve that has the minimum distance to the center of mass (COM) of the formation. We call this point the closest point. The robot then estimates the tangent vector to the curve and the curvature at this closest point. These information will be used to estimate the orientation and the position of the formation relative to the curve.

Let θ_i be the angle between the horizontal axis of the ith frame and the tangent vector to the boundary at the closest point to the COM. We use $\mathbf{R}_{ji}$ to represent the relative displacement vector between robot j and i, measured in the ith frame. The entire formation can now be viewed as a deformable body. The state of the deformable body is described by three variables $(\mathbf{R}_{ic}, g_i, \mathbf{s})$: $\mathbf{R}_{ic}$ indicates the position of the center of mass i.e.

$$\mathbf{R}_{ic} = \frac{1}{N}\sum_{j\neq i}\mathbf{R}_{ji}\,, \tag{1}$$

$g_i = \begin{bmatrix} \cos\theta_i & \sin\theta_i \\ -\sin\theta_i & \cos\theta_i \end{bmatrix}$ describes the spatial orientation, and $\mathbf{s}$ is a vector of shape variables. Such shape variables must be independent of the orientation and position of the formation. For example, the mutual distances between particles can serve as shape variables c.f. our previous work [15] and the reference [13]. To describe a planar formation with N particles, altogether $(2N-3)$ shape variables are required i.e. $\mathbf{s} = [s_1, s_2, ..., s_{2N-3}]^T$. Figure 1 shows a set of shape variables for triangular formations.

Let d_c be the distance between the COM and the closest point. In order to determine the relative position of the COM to the boundary curve and the formation orientation, we propose the following algorithm:

Algorithm 1 Find d_c and θ_i on the ith robot.

On the ith robot, perform the following procedures:

1) For $j = 1,2,...,N$ and $j \neq i$, measure the relative displacement vectors $\mathbf{R}_{ji}$ between robots j and i in the ith frame.
2) Estimate the COM position $\mathbf{R}_{ic} = \frac{1}{N}\sum_{j\neq i}\mathbf{R}_{ji}$.
3) For each value of α, find the intersection point, $\mathbf{R}_I(\alpha)$, between the sensor ray indexed by α and the boundary curve.
4) Estimate $d_i(\alpha) = \| \mathbf{R}_{ic} - \mathbf{R}_I(\alpha) \|$, the distance between the estimated COM and the intersection point $\mathbf{R}_I(\alpha)$.
5) Determine a candidate for the closest point by finding $\alpha^i_{\min}$ and $d^i_{\min}$:
$$d^i_{\min} = \min_\alpha\{d_i(\alpha)\}$$
$$\alpha^i_{\min} = \arg\left(\min_\alpha\{d_i(\alpha)\}\right)\,. \tag{2}$$
6) For $j = 1,2,...,N$ and $j \neq i$, find the relative angle β_{ji} between the two vectors $\mathbf{R}_I(\alpha^i_{\min})$ and $\mathbf{R}_{ji}$.
7) For $j = 1,2,...,N$ and $j \neq i$, send $(d^i_{\min}, \beta_{ji})$ to robot j.
8) Gather $d^j_{\min}$ and β_{ij} from other robots. Note β_{ij} indicates that the angle comes from robot j. Find index k and the minimum distance d_c as
$$k = \arg\left(\min_i\{d^i_{\min}\}\right)$$
$$d_c = d^k_{\min}. \tag{3}$$
9) If $k = i$, then the closest point is at $\mathbf{R}_o = \mathbf{R}_I(\alpha^i_{\min})$. If $k \neq i$, then the closest point is at
$$\mathbf{R}_o = -\mathbf{R}_{ki} + d_c\cos\beta_{ik}\frac{\mathbf{R}_{ki}}{\|\mathbf{R}_{ki}\|} + d_c\sin\beta_{ik}\mathbf{R}^\perp_{ki} \tag{4}$$
where $\mathbf{R}^\perp_{ki}$ is the unit vector that is perpendicular to $\mathbf{R}_{ki}$ with a leading angle of 90°.
10) Estimate the tangent vector and the curvature at the closest point using, for example, algorithms in [15]. This produces estimates θ_i and κ_c

We define the size of a formation as

$$Z = \left(\|\mathbf{R}_{ic}\|^2 + \sum_{j\neq i}^{N}\|\mathbf{R}_{ji} - \mathbf{R}_{ic}\|^2\right)^{\frac{1}{2}}.$$

It is true that as long as the size of the formation is less than the distance between the closest point and the center of mass i.e. $Z < d_c$, the closest point can always be detected by any of the robots. To see this, imagine a disc with radius d_c centered at the COM. The closest point, hence the entire obstacle, is located outside the disc. We now draw the second disc centered at the COM but with radius Z. Then the disc with radius Z lies within the disc with radius d_c. Any line between any robot and the closest point lies entirely inside the bigger disc, hence is not blocked by any portion of the

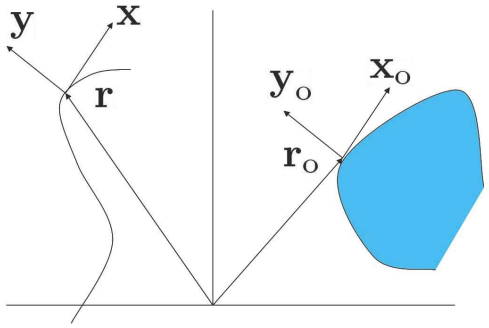

Fig. 2. The moving frames attached to a particle $\mathbf{r}$ and the closest point $\mathbf{r}_o$.

obstacle. Therefore, since all robots are considered to be ideal points, the closest point is detectable by all robots.

Therefore, the steps 6)–9) in algorithm 1 for determining the closest point via communications are redundant when the formation is small. However, in reality, the sensors all have limited range, the robots often have significant size and the boundary curve of an object is not always smooth. We need such redundancy to make sure the closest point is always well-determined.

To describe velocities, we use $\mathbf{V}_{ic}$ for the velocity of the center of mass, Ω_i for the angular velocity of the body and $\dot{\mathbf{s}}$ for shape changes over time.

To estimate the velocity $\mathbf{V}_{ic}$, we have $\mathbf{V}_{ic} = \dot{\mathbf{R}}_i + \dot{\mathbf{R}}_{ic}$ where $\dot{\mathbf{R}}_i$ is the velocity of robot i in its chosen coordinate system. The length of $\dot{\mathbf{R}}_i$ is the speed and is measured by the speedometer. We need to determine the direction of $\dot{\mathbf{R}}_i$. It is necessary to use the equations that govern the relative motion between a particle (robot) and the boundary curve. These equations are established in [17]. Here we outline the necessary steps.

Let $\gamma > 0$ be the non-zero speed of a particle. We can construct a right-handed moving frame at the particle using the unit velocity vector $\mathbf{x} = \frac{\dot{\mathbf{r}}}{\gamma}$ and a uniquely determined unit normal vector $\mathbf{y}$ to form a right handed coordinate frame with $\mathbf{x}$, as shown in Figure 2. We introduce a steering control $u = \frac{1}{\gamma^2}\mathbf{f}\cdot\mathbf{y}$ and a speed control $v = \mathbf{f}\cdot\mathbf{x}$ where $\mathbf{f}$ is the total force applied to the particle.

On the smooth, closed boundary curve of a planar object, we can always find a point which has the minimum distance to the particle. Let $\mathbf{r}_o$ denote the position of this closest point on the boundary curve. The tangent vector $\mathbf{x}_o$ and the normal vector $\mathbf{y}_o$ at this point forms a right-handed frame moving with this point when the particle moves. Let ϕ denote the angle between $\mathbf{x}$ and $\mathbf{x}_o$ so that

$$\cos\phi = \langle \mathbf{x}_o, \mathbf{x}\rangle \text{ and } \sin\phi = \langle \mathbf{x}_o, \mathbf{y}\rangle \ . \tag{5}$$

Let $d = \| \mathbf{r} - \mathbf{r}_o \|$. Then in [17], we found

$$\begin{aligned} \dot{d} &= -\mathrm{S}_n \gamma \sin(\phi) \\ \dot{\phi} &= \gamma\left(\frac{\kappa\cos(\phi)}{1 \pm |\kappa| d} - u\right) \\ \dot{\gamma} &= v. \end{aligned} \tag{6}$$

where $\mathrm{S}_n = \mathrm{sign}(\langle \mathbf{r} - \mathbf{r}_o, \mathbf{y}_o\rangle)$ which assume constant $+1$ or -1, depending on the choice for the direction of the curve.

We use the first equation in (6) to estimate the direction of the velocity of the particle.

Algorithm 2 On the ith robot, estimate $\mathbf{V}_{ic}$, the velocity of the COM.

1) Measure $\dot{\mathbf{R}}_{ji}$ for $j = 1,2,...,N$ and $j \neq i$.
2) Measure the angle ϕ_i between $\dot{\mathbf{R}}_i$ and the tangent vector to the boundary at the closest point to robot i using $\phi_i = \arcsin(\frac{\dot{d}_i}{S_n \gamma_i})$ where $\dot{d}_i$ is the rate of change for the distance between robot i and its closest point and γ_i is the speed of robot i.
3) Find the velocity $\mathbf{V}_{ic} = \dot{\mathbf{R}}_i + \frac{1}{N}\sum_{j\neq i}^{N} \dot{\mathbf{R}}_{ji}$.

After $\mathbf{V}_{ic}$ is known, we can also find ϕ_c that is the angle between $\mathbf{V}_{ic}$ and the tangent vector to the boundary at the closest point to the COM.

In the planar setting, the angular velocity will always be perpendicular to the plane. For each robot, the angular speed Ω_{iz} can be estimated as

$$\Omega_{iz} = \dot{\theta}_i + \| \mathbf{V}_{ic} \| \cos(\phi_c) \frac{\kappa_c}{1 \pm |\kappa_c| d_c}. \tag{7}$$

All robots will agree on the measurements of shape variables $\mathbf{s}$ and the rate of change for those shape variables $\dot{\mathbf{s}}$. On the other hand, the measurements for the orientation g_i (i.e. θ_i) and angular velocity Ω_i depend on how the robot establishes the body coordinate frame. Different robots may not always agree on each other because the angles between displacement vectors may change over time. This phenomena is called gauge dependence.

The angular velocity Ω_i needs to be adjusted so that all robots will agree on an estimate of the rotational motion of the formation. In [18], we define the gauge covariant angular velocity as $\Upsilon = \Omega_i + \mathbf{A}\dot{\mathbf{s}}$ where $\mathbf{A}$, called the collection of vector potentials, is a matrix that depends on the shape variables $\mathbf{s}$. The procedure to compute $\mathbf{A}$ can also be found in [18].

III. Controlled Dynamics

In the lab fixed coordinate frame, each particle satisfies the second order Newton's equation: $\ddot{\mathbf{r}}_i = \mathbf{f}_i$ where $\mathbf{f}_i$ represents the total force on particle i for $i = 1,2,...N$. The formation control problem when the measurements for positions $\mathbf{r}_i$ are available has been studied intensively using graph theoretic method ,c.f. [19]–[22], to name only a few.

Without the GPS, the dynamics of the formation–viewed as a deformable body–can be studied as a controlled Lagrangian system. The Lagrange-D'Alembert principle is applied to derive the dynamics which are described by the following equations:

1) the equation for the center of mass, $\mathbf{r}_c = \frac{1}{N}\sum_{i=1}^{N} \mathbf{r}_i$, in lab frame is

$$N\ddot{\mathbf{r}}_c = \mathbf{f}_c \tag{8}$$

where $\mathbf{f}_c$ is the combined force on the center of mass;

2) the equations for shape change and rotation are

$$\frac{d}{dt}(I\Upsilon) = -\Omega \times I\Upsilon + \mathbf{u}_g \,, \tag{9}$$

$$\begin{aligned}\frac{d}{dt}(G\dot{\mathbf{s}}) + \mathbf{A}^T \frac{d}{dt}(I\Upsilon) &= \frac{1}{2}[\frac{\partial I}{\partial \mathbf{s}}]^* : (\Upsilon, \Upsilon) \\ &+ ([\frac{\partial \mathbf{A}}{\partial \mathbf{s}}]^* - [\frac{\partial \mathbf{A}}{\partial \mathbf{s}}])(\dot{\mathbf{s}}, I\Upsilon) \\ &+ \frac{1}{2}[\frac{\partial G}{\partial \mathbf{s}}]^*(\dot{\mathbf{s}}, \dot{\mathbf{s}}) + \mathbf{u}_s, \end{aligned} \tag{10}$$

where I is the locked inertia tensor, G is a metric tensor on shape space and $\mathbf{A}$ is the collection of vector potentials. All these tensors are functions of shape variables as shown in [18].

In equations (9) and (10), $[\frac{\partial I}{\partial \mathbf{s}}]$, $[\frac{\partial G}{\partial \mathbf{s}}]$ and $[\frac{\partial \mathbf{A}}{\partial \mathbf{s}}]$ are third order tensors obtained by taking the Frechet derivatives of the tensors I,G and $\mathbf{A}$ with respect to vector $\mathbf{s}$, $[\frac{\partial I}{\partial \mathbf{s}}]^*$, $[\frac{\partial G}{\partial \mathbf{s}}]^*$ and $[\frac{\partial \mathbf{A}}{\partial \mathbf{s}}]^*$ are the cyclic transpose of these third order tensors, c.f. [23], and $(\mathbf{u}_g, \mathbf{u}_s)$ are controls for rotation and shape changes.

Equation (8) still requires the position $\mathbf{r}_c$ in the lab coordinate frame. In stead of using (8), we use the following set of equations, which are similar to (6), to describe the relative movement between the COM and the boundary curve

$$\begin{aligned} \dot{d_{\mathrm{c}}} &= -\mathrm{S}_n \gamma_{\mathrm{c}} \sin(\phi_{\mathrm{c}}) \\ \dot{\phi_{\mathrm{c}}} &= \gamma_{\mathrm{c}} \left(\frac{\kappa_{\mathrm{c}} \cos(\phi_{\mathrm{c}})}{1 \pm |\kappa_{\mathrm{c}}| d_{\mathrm{c}}} - u_{\mathrm{c}} \right) \\ \dot{\gamma_{\mathrm{c}}} &= v_{\mathrm{c}}. \end{aligned} \tag{11}$$

Here we view the COM as one particle. Equations (11) are derived by following the same procedure for a generic particle. We use the subscript "c" to indicate that the variables are defined for the COM and its closest point on the boundary curve. Hence γ_{c} represents the speed of the COM, u_{c} is the steering control for the COM, and v_{c} is the speed control of the COM.

Therefore, equations (9), (10), and (11) are the system dynamics for the entire formation observed by each robot in its own choice of body coordinate frame. All quantities in these equations can be estimated by the robot using range sensors and a speedometer.

IV. Controller Design

We want to control the entire formation to move along the boundary curve in desired formation. Suppose the desired shape of the formation is given by $\mathbf{s}^0$ and the desired distance between the COM and the boundary curve is given by d^0. The goal is to design feedback controls $(\mathbf{u}_g, \mathbf{u}_s, u_{\mathrm{c}}, v_{\mathrm{c}})$ so that as $t \to +\infty$, the controlled dynamics achieve $\mathbf{s} \to \mathbf{s}^0$ and $d_{\mathrm{c}} \to d^0$. Meanwhile, we want to avoid collisions between particles and between any particle and the boundary curve.

The speed of the COM can be stabilized at the unit speed by the controller $v_{\mathrm{c}} = -k_1(\gamma_{\mathrm{c}} - 1)$ where $k_1 > 0$ determines the convergent speed. From now on we assume that the speed of the COM $\gamma_{\mathrm{c}} = 1$.

In order to avoid collision with the boundary, we want the distance between any particle and the COM to be always less than the distance between the COM and the closest point on the boundary curve. This can be written as a sufficient condition:

$$\max_i \{ \| \mathbf{r}_i(t) - \mathbf{r}_c(t) \| \} < d_{\mathrm{c}}(t) \tag{12}$$

for all $t > 0$. If $Z(\mathbf{s}(t)) < d_{\mathrm{c}}(t)$, then condition (12) is satisfied.

We define $w = d_{\mathrm{c}} - Z(\mathbf{s})$ and construct a smooth function $\hbar(w)$ with its derivative $\widetilde{f}(w) = \hbar'(w)$ satisfying the following conditions:

(A1) $\hbar(w) \geq 0$ for $w \in (0, +\infty)$ where $\hbar(w) = 0$ if and only if $w = d^0 - Z(\mathbf{s}^0)$;
(A2) $\hbar(0) \to +\infty$ and $\hbar(+\infty) \to +\infty$;
(A3) $\widetilde{f}(w) = 0$ if and only if $w = d^0 - Z(\mathbf{s}^0)$.

We introduce a Lyapunov candidate function

$$V_{\mathrm{A}} = \hbar(w) - 2\log(\cos(\frac{\phi_{\mathrm{c}}}{2})) + V_{\mathrm{L}}. \tag{13}$$

where V_{L} is the following function:

$$V_{\mathrm{L}} = \frac{1}{2} \sum_{i=1}^{2N-3} h_i(s_i) + \frac{1}{2} \Upsilon^T I \Upsilon + \frac{1}{2} \dot{\mathbf{s}}^T G \dot{\mathbf{s}} \tag{14}$$

with each $h_i(s_i)$ being a smooth function of a shape variable s_i and satisfying the following conditions:

(A4) $h_i(s_i)$ assumes its minimum when $s_i = s_i^0$;
(A5) $\lim_{s_i \to 0} h_i(s_i) = +\infty$;
(A6) let $f_i(s_i) = h_i'(s_i)$, then $f_i(s_i) = 0$ if and only if $s_i = s_i^0$.

To compute the time derivative of V_{A} along the controlled dynamics, we first compute the derivative of each term in the right hand side of equation (13). For the first term we have

$$\begin{aligned} \dot{\hbar}(w) &= \widetilde{f}(w) \left(-\dot{Z} + \dot{d_{\mathrm{c}}} \right) \\ &= -\widetilde{f}(w) \left(\frac{\partial Z}{\partial \mathbf{s}} \dot{\mathbf{s}} + \mathrm{S}_n \sin(\phi_{\mathrm{c}}) \right) . \end{aligned} \tag{15}$$

For the second term we have

$$\begin{aligned} \frac{d}{dt} \left(-2\log(\cos\frac{\phi_{\mathrm{c}}}{2}) \right) &= \frac{\sin(\frac{\phi_{\mathrm{c}}}{2})}{\cos(\frac{\phi_{\mathrm{c}}}{2})} \dot{\phi}_{\mathrm{c}} \\ &= \frac{\sin(\frac{\phi_{\mathrm{c}}}{2})}{\cos(\frac{\phi_{\mathrm{c}}}{2})} \left(\frac{\kappa_{\mathrm{c}} \cos\phi_{\mathrm{c}}}{1 \pm |\kappa_{\mathrm{c}}| d_{\mathrm{c}}} - u_{\mathrm{c}} \right) . \end{aligned} \tag{16}$$

For the third term, let $\mathbf{F}(\mathbf{s})$ be a vector function such that $\mathbf{F}_i(\mathbf{s}) = f_i(s_i)$. The time derivative of function V_{L} is

$$\begin{aligned} \dot{V}_{\mathrm{L}} &= \langle \mathbf{F}(\mathbf{s}), \dot{\mathbf{s}} \rangle + \langle \Omega, \mathbf{u}_g \rangle + \langle \dot{\mathbf{s}}, \mathbf{u}_s \rangle \\ &= \langle \dot{\mathbf{s}}, \mathbf{u}_s + \mathbf{F}(\mathbf{s}) \rangle + \langle \Omega, \mathbf{u}_g \rangle \end{aligned} \tag{17}$$

where we use $\langle \ , \ \rangle$ to denote the inner product.

Therefore, the time derivative for V_{A} is

$$\begin{aligned} \dot{V}_{\mathrm{A}} = &\frac{\sin(\frac{\phi_{\mathrm{c}}}{2})}{\cos(\frac{\phi_{\mathrm{c}}}{2})} \left(\frac{\kappa_{\mathrm{c}} \cos\phi_{\mathrm{c}}}{1 \pm |\kappa_{\mathrm{c}}| d_{\mathrm{c}}} - 2\mathrm{S}_n \cos^2(\frac{\phi_{\mathrm{c}}}{2}) \widetilde{f}(w) - u_{\mathrm{c}} \right) \\ &+ \left\langle \dot{\mathbf{s}}, \mathbf{u}_s + \mathbf{F}(\mathbf{s}) - \widetilde{f}(w) \left(\frac{\partial Z}{\partial \mathbf{s}} \right)^T \right\rangle + \langle \Omega, \mathbf{u}_g \rangle . \end{aligned} \tag{18}$$

We design the control laws to be

$$u_c = \frac{\kappa_c \cos\phi_c}{1 \pm |\kappa_c| d_c} - 2S_n \cos^2(\frac{\phi_c}{2}) \widetilde{f}(w) + k_2 \sin(\frac{\phi_c}{2})$$
$$\mathbf{u}_g = -k_3 \Upsilon$$
$$\mathbf{u}_s = -\mathbf{F}(\mathbf{s}) - k_3 \dot{\mathbf{s}} - k_3 \mathbf{A}^T \Upsilon + \widetilde{f}(w) \left(\frac{\partial Z}{\partial \mathbf{s}} \right)^T . \quad (19)$$

where k_2, $k_3 > 0$. This results in

$$\dot{V}_A = -\frac{\sin^2(\frac{\phi_c}{2})}{\cos(\frac{\phi_c}{2})} - k_3 \| \Upsilon \|^2 - k_3 \| \dot{\mathbf{s}} \|^2 . \quad (20)$$

As one can see, this derivative is not greater than zero. In order for $\dot{V}_A = 0$ we must have the following equations satisfied:

$$\Omega = 0, \ \dot{\mathbf{s}} = 0, \text{ and } \sin(\frac{\phi_c}{2}) = 0 . \quad (21)$$

Theorem 4.1: Suppose there is one smooth boundary curve in the workspace of a robot formation. Suppose the initial states of the formation satisfy $\cos(\frac{\phi_c(t_0)}{2}) \neq 0$ and $Z(\mathbf{s}(t_0)) < d_c(t_0)$. Suppose the desired shape of the formation is given by $\mathbf{s}^0$ and the desired distance between the COM and the boundary curve is given by d^0 such that the size $Z(\mathbf{s}^0) < d^0$. Then under the control laws (19) , the following statements hold:

1) The shape of the formation converges i.e. $\mathbf{s}(t) \to \mathbf{s}^0$ as $t \to +\infty$.
2) The distance between the COM and the boundary curve converges, i.e. $d_c(t) \to d^0$ as $t \to +\infty$.
3) No collision will happen between any pair of particles or between any particle and the boundary curve.

Proof: By LaSalle's invariance principle, the dynamics for the state variables $(\phi_c, d_c, \mathbf{s}, \dot{\mathbf{s}}, \dot{\Omega})$ converge to the maximal invariant set within the set M_1 where (21) are satisfied. On this set M_1, the closed loop system equations are simplified to

$$\dot{d}_c = -S_n \sin(\phi_c) = 0$$
$$\dot{\phi}_c = 2S_n \widetilde{f}(w)$$
$$I(\dot{\Omega} + \mathbf{A}\ddot{\mathbf{s}}) = 0$$
$$G\ddot{\mathbf{s}} = -\mathbf{F}(\mathbf{s}) + \widetilde{f}(w) \left(\frac{\partial Z}{\partial \mathbf{s}} \right)^T . \quad (22)$$

Then on the invariant set, we must have $\dot{\phi}_c$,$\dot{\Omega}$ and $\ddot{\mathbf{s}}$ all vanish. Therefore we conclude that on the maximal invariant set $\widetilde{f}(w) = 0$ and $\mathbf{F}(\mathbf{s}) = 0$. This, together with $\sin(\frac{\phi_c}{2}) = 0$, prove the convergence results.

If at any time instance, $Z(t)$ is near $d_c(t)$, then condition (A2) provides that $\hbar(w) \to \infty$, hence $V_A \to \infty$. Because initially $Z(t_0) < d_c(t_0)$, then the initial value of the Lyapunov function V_A is finite. Since the value of the Lyapunov function is not increasing, it is guaranteed that $Z(t) < d_c(t)$ for all $t > t_0$. Therefore, no collision can happen between any robot and the boundary curve.

If collision between a pair of particles is about to happen, we must have $s_i \to 0$ for some shape variable s_i. Therefore $h_i(s_i) \to \infty$. Hence if initially there is no collision between any pair of particles i.e. $h_i(s_i)$ is finite, then no collision can happen at any time t. If at any time instance $\cos(\frac{\phi_c(t)}{2}) = 0$, then the Lyapunov function V_A goes to infinity. Therefore, if initially $\cos(\frac{\phi_c(t_0)}{2}) \neq 0$, then $\cos(\frac{\phi_c(t)}{2}) \neq 0$ for all $t > t_0$. ■

TABLE I

INITIAL POSITION AND VELOCITY FOR THE THREE PARTICLES

Particle	Position	Velocity
1	$(-14, 1)$	$(1, 0)$
2	$(-14, -1)$	$(1, 0)$
3	$(-13, 0)$	$(1, 0)$

TABLE II

PLANS FOR THE FORMATION AROUND AN ELLIPTIC BOUNDARY

Time(s)	s_1	s_2	s_3	Size(Z)	Separation(d_c)
0-8	1	1	$\pi/3$	1	1.3
8-14	0.6	1.2	$\pi/3$	0.98	1.28
14-20	2	2	$\pi/3$	2	2.3
20-26	1	2	$\pi/5$	1.50	1.80
26-30	0.6	0.6	$\pi/3$	0.6	0.9

V. SIMULATION RESULTS

We present simulation results in MATLAB to demonstrate the tracking behavior. We show here a formation of three robots (particles) in the workspace with one obstacle that has elliptic boundary. Table I shows the initial position and velocity of the three particles. Although the states are given in a lab coordinate frame, This information is not available to the robots. Instead, the robots use their range sensors and speedometer to measure the shape, orientation and position of the formation relative to the boundary ellipse.

We choose a set of three shape variables as shown in Figure 1. Variable s_1 is the distance between particle 1 and 2, s_2 is the distance between particle 1 and 3, and s_3 is the angle between the two displacement vectors $\mathbf{r}_{12}$ and $\mathbf{r}_{13}$. Note that our methods do not depend on the choice of shape variables. For example, we can also let s_3 be the distance between particle 1 and 3. The convergence results still hold.

We designed a motion plan to perform shape changes while the formation is moving around the elliptic obstacle. The plan is shown in Table II. All data in the table are the desired values which define the shape of the formation and the distance between the center of mass and the closest point. For example, in time between 0 and 8 seconds, we want the shape of the formation to be a equilateral triangle with each side having unit length. Initially, all three particles are outside the boundary and there is no collision between particles and the boundary ellipse. To guarantee safe operation for all time, we want $d_c(t) - Z(\mathbf{s}(t)) = 0.3$.

After the plan is executed, we analyze the data and plot the change of the data over time. Figure 3 shows the trajectory of the center and the configuration of the formation at points along the trajectory. It is intuitive that there is no collision and the formation shape is as desired.

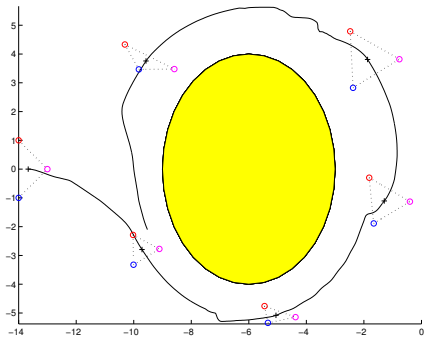

Fig. 3. Motion and shape changes of the three-robot formation tracking an elliptic boundary

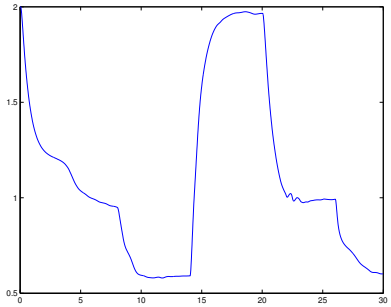

Fig. 4. Convergence of shape variable s_1 as a function of time.

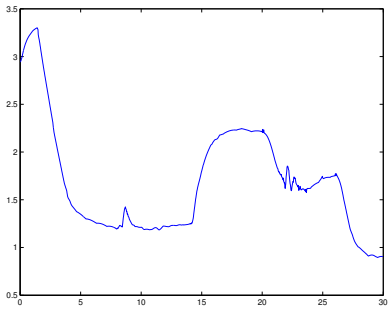

Fig. 5. Convergence of d_c, the distance between the COM and the boundary .

The convergence of one shape variable is shown in Figure 4. The other two shape variables are not shown due to space limitation. As we can see, shape changes are desired at time instances 8, 14, 20, and 26. The shape variables converges to the desired value each time a shape change is desired. The boundary tracking performance is shown in Figure 5. We see the distance between the closest point and the center converges to the desired values.

VI. Summary and Future Work

We develop a method for robot formations to perform shape changes while following a boundary curve. We have shown that no GPS is required if each robot is equipped with range sensors and a speedometer. Future work may include study of how the algorithm scales to additional agents, how measurement noise affects performance, and how reduced communication or communication delays between robots affect the results.

References

[1] V. J. Lumelsky and A. Stepanov, "Path planning strategies for a point mobile automaton moving amidst unknown obstacles of arbitrary shape," *Algorithmica*, vol. 2, pp. 403–430, 1987.

[2] Z. Shiller, "Online suboptimal obstacle avoidance," *The International Journal of Robotics Research*, vol. 19, no. 5, pp. 480–497, 2000.

[3] I. Kamon, E. Rimon, and E. Rivlin, "Range-sensor-based navigation in three dimensional polyhedral environments," *International Journal of Robotics Research*, vol. 20, no. 1, pp. 6–25, 2001.

[4] P. Ogren and N. E. Leonard, "Obstacle avoidance in formation," in *Proc. of IEEE International Conference on Robotics and Automation*, 2003, pp. 2492–2497.

[5] D. Chang, S. Shadden, J. Marsden, and R. Olfati-Saber, "Collision avoidance for multiple agent systems," in *Proc. 42nd IEEE Conference on Decision and Control*, Dec. 2003, pp. 539–543.

[6] L.-F. Lee, R. M. Bhatt, and V. Krovi, "Comparison of alternate methods for distributed motion planning of robot collectives within a potential-field framework," in *Proc. of 2005 IEEE International Conf. on Robotics and Automation*, Barcelona, Spain, 2005, pp. 99–104.

[7] G. J. Toussaint, P. D. Lima, and D. J. Pack, "Localizing rf targets with cooperative unmanned aerial vehicles," in *Proceedings of 2007 American Control Conference*, New York, New York, 2007, pp. 5928–5933.

[8] O. Lefebvre and F. Lamiraux, "Localization and trajectory following for multi-body wheeled mobile robots," in *Proc. of 2007 IEEE International Conf. on Robotics and Automation*, Rome, Italy, 2007, pp. 3086–3091.

[9] S. Mastellone, D. M. Stipanovic, and M. W. Spong, "Remote formation control and collision avoidance for multi-agent nonholonomic systems," in *Proc. of 2007 IEEE International Conference on Robotics and Automation*, Rome, Italy, 2007, pp. 1062–1067.

[10] D. Cruz, J. McClintock, B. Perteet, O. Orqueda, Y. Cao, and R. Fierro, "Decentralized cooperative control: A multivehicle platform for research in networked embedded systems," *IEEE Control Systems Magazine*, vol. 27, no. 3, pp. 58–78, 2007.

[11] D. G. Kendall, "Shape manifolds, procrustean metrics, and complex projective spaces," *Bulletin of London Math. Society*, vol. 16, pp. 81–121, 1984.

[12] ——, "A survey of the statistical theory of shape(with discussion)," *Statistical Science*, vol. 4, pp. 87–120, 1989.

[13] R. Littlejohn and M. Reinsch, "Internal or shape coordinates in the *n*-body problem," *Physical Review A*, vol. 52, no. 3, pp. 2035–2051, 1995.

[14] ——, "Gauge fields in the separation of rotation and internal motions in the n-body problem," *Reviews of Modern Physics*, vol. 69, no. 1, pp. 213–275, 1997.

[15] F. Zhang, M. Goldgeier, and P. S. Krishnaprasad, "Control of small formations using shape coordinates," in *Proc. of 2003 International Conf. of Robotics and Automation*. Taipei, Taiwan: IEEE, 2003, pp. 2510–2515.

[16] C. Belta and V. Kumar, "Abstraction and control for groups of robots," *IEEE Trans. on Robotics*, vol. 20, no. 5, pp. 865–875, 2004.

[17] F. Zhang, E. Justh, and P. S. Krishnaprasad, "Boundary following using gyroscopic control," in *Proc. of 43rd IEEE Conf. on Decision and Control*, Atlantis, Paradise Island, Bahamas, 2004, pp. 5204–5209.

[18] F. Zhang, "Geometric cooperative control of formations," Ph.D. dissertation, ISR Technical Report PHD2004-5, University of Maryland, 2004.

[19] A. Jadbabaie, J. Lin, and A. S. Morse, "Coordination of groups of mobile agents using nearest neighbor rules," *IEEE Trans. on Automatic Control*, vol. 48, no. 6, pp. 988–1001, 2003.

[20] W. Ren and R. W. Beard, "Consensus seeking in multi-agent systems under dynamically changing interaction topologies," *IEEE Trans. on Automatic Control*, vol. 50, no. 5, pp. 655–661, 2005.

[21] R. Olfati-Saber and R. M. Murray, "Consensus problems in networks of agents with switching topology and time-delays," *IEEE Trans. on Automatic Control*, vol. 49, no. 9, pp. 1520–1533, 2004.

[22] R. Sepulchre, D. Paley, and N. E. Leonard, "Stabilization of planar collective motion, part I: All-to-all communication," *IEEE Trans. on Automatic Control*, 2006.

[23] S. S. Antman, *Nonlinear problems of elasticity*. New York: Springer-Verlag, 1995.